Astron. Astrophys. 327, 1177–1184 (1997)

ASTRONOMY
AND
ASTROPHYSICS

Kinematics and electron temperatures in the core of Orion A⋆

T.L. Wilson, L. Filges, C. Codella, W. Reich, and P. Reich

Max-Planck-Institut für Radioastronomie, Auf dem Hügel 69, D-53121 Bonn, Germany

Received 23 May 1997 / Accepted 11 July 1997

Abstract. A map of the core of Orion A, with a 42″ resolution in the 64α recombination line of hydrogen, covering $\sim$5′ by $\sim$5′, is presented. The $V_{\rm lsr}$ distribution shows a complex variation about the center of the ionized gas emission: From $\Delta\alpha$=-200″ to +300″, the $V_{\rm lsr}$ varies from -5km s^{-1} to +2km s^{-1} then to -4km s^{-1}, finally rising to +3km s^{-1}. A search for cold ($T_{\rm e}$ $\sim$3000K) ionized gas toward the KL nebula has revealed no measurable differences in $T_{\rm e}$ between this region and other parts of Orion A. The average $T_{\rm e}$ from our data is 8300$\pm$200K. We find *no* significant difference between $T_{\rm e}$ values determined from radio recombination lines and those determined from forbidden optical lines of [O III], although the $T_{\rm e}$ value from Balmer decrement data is markedly lower. The turbulent velocity varies by $<$5% over the region mapped. On the basis of our 2.45′ resolution, high dynamic range 6 cm continuum map, we find that the emission falls off faster in the East than in the West. We find support for the model in which Orion A is ionization bounded in the East but density bounded in the West. The ionized gas in the West is flowing in the direction of the Sun, while the more positive $V_{\rm lsr}$ values in the east may be caused by the flow of ionized gas off the foreground Dark Bay. This ionized region may have little fine scale structure, since there is little continuum emission in interferometer maps.

Key words: ISM: Orion A – ISM: H II regions – ISM: kinematics and dynamics – ISM: structure – radio lines: ISM

1. Introduction

The Orion Nebula is the most studied HII region/molecular cloud complex in the Galaxy. The foreground HII region Orion A (=M42=NGC1976) has been extensively studied in the optical and mapped in the radio continuum with an angular resolution extending down to 0.1″ (see, e.g., Felli et al. 1993). Maps in radio recombination lines have the advantage of being unaffected by extinction in foreground material or in the HII region itself. Radio recombination line data for H, He and C, with angular resolutions of 2.6′ (Jaffe & Pankonin 1978), 1.3′ (Kuiper & Evans 1978), 1′ (Pankonin et al. 1979) and 42″ (Pauls & Wilson 1977) have been made. Optical determinations of $T_{\rm e}$ have been made by Peimbert & Torres-Peimbert (1977), with emphasis on the determination of element abundances; measurements of the optical recombination line of oxygen have been carried out by Osterbrock et al. (1992) and Peimbert et al. (1993).

Models of the distribution of electron temperature based on radio data have been proposed by Brocklehurst & Seaton (1972), Lockman & Brown (1975), Shaver (1980) and Wilson & Jäger (1987). The models of Shaver (1980) and Wilson & Jäger (1987) are similar in that both require electron densities, $N_{\rm e}$, which are much larger than the RMS values obtained from radio continuum measurements and geometry. The most complex model is that of Wilson & Jäger (1987), which shows the best agreement with measurements. In this model, $T_{\rm e}$ decreases from 8500K to $\sim$6500K and N_e from $1.2 \cdot 10^4$ cm^{-3} to 300 cm^{-3} with increasing distance from the exciting stars. The most important influence on the value of $T_{\rm e}$ is the cooling of the ionized gas via fine structure line radiation from oxygen, carbon and nitrogen: At higher N_e, these lines are collisionally deexcited, and $T_{\rm e}$ remains high, while further from the core of Orion A, where N_e is lower, the gas can cool more efficiently, so that $T_{\rm e}$ is lower.

Interest in the Orion HII region has been reawakened by observations using the Hubble Space Telescope (hereafter HST; see, e.g., O'Dell et al. 1993), as well as other high angular resolution studies (Pogge et al. 1992, Hayward et al. 1994, McCaughrean & Stauffer 1994). The basic physics underlying the 3 dimensional model of Wen & O'Dell (1995) is similar to that used in models proposed to explain the radio recombination line and free-free continuum emission, since this emission *must* arise from a thin layer adjacent to the neutral gas boundary (Shaver 1980; Wilson & Jäger 1987). Although our angular resolution is considerably worse than the optical studies, the data are complementary and allow an extension of the studies of $T_{\rm e}$ determinations and dynamics of the core of Orion A, even in regions of high extinction. With a single telescope, all of the flux density will be recorded, so that there will be no ambiguity in interpretations on account of missing flux density caused by structural information which is not recorded by the interferometer. For example, the VLA map of Orion A made by Johnston et al. (1983)

Send offprint requests to: T.L. Wilson

⋆ Table 1 is only available in electronic form at the CDS (Strasbourg) via anonymous ftp to cdsarc.u-strasbg.fr (130.79.128.5) or via http://cdsweb.u-strasbg.fr/Abstract.html

contained a total continuum flux density of ∼90 Jy, ∼25% of the total. In order to obtain a finer sampling of the ionized gas, we have chosen to measure the H64α line with the 100-m telescope of the MPIfR at 23 GHz, with an angular resolution of ∼42″. We have adopted 500 pc for the distance to Orion A. At this distance, 42″ is equivalent to 0.1 pc. Previous single radio telescope maps of limited regions in radio recombination lines have been made with similar resolutions (Pauls & Wilson 1977, Hasegawa & Akabane 1984). The goals of this new, more extensive mapping program are twofold: (1) Measure the distribution of radial velocities over the core of Orion A, in order to obtain radial velocity and linewidth data and (2) Determine the electron temperatures (both the LTE values, $T_{\rm e}^*$ and actual values $T_{\rm e}$) over the entire core region. These $T_{\rm e}$ results can be used to check corrections to oxygen abundance determinations. In addition, we present a high dynamic range continuum map, made at 6cm, to determine the fall off of the free–free emission as a function of distance from the Trapezium.

2. Observations and results

2.1. H64α line data

The H64α line and continuum data were taken with the 100-m telescope of the MPIfR. The receiver was a K-band maser together with a 1024 channel autocorrelation spectrometer used as a single receiver. The total bandwidth used was 25 MHz. This gave a velocity resolution of 0.76 km s^{-1} in each channel. Our data were Hanning smoothed to obtain a velocity resolution of 1.4 km s^{-1}. The total velocity coverage was 320 km s^{-1}. The data were taken only under excellent weather conditions; the system noise temperature on cold sky was less than 100K. The observing procedure employed was as follows. First, four to five measurements of the continuum intensities were made by rapid scanning in Right Ascension, using measurements of the total power continuum, that is, without any switching arrangement (for this reason, data could be taken only in excellent weather). Then spectra were taken employing position switching for about 2-3 hours. The on-source integration time was 1 minute, while the time spent on the off-source reference position was 3 minutes. Usually, three on-source spectra were taken for each reference spectrum. In all, 261 on-source positions were measured. The reference position was taken at -5 minutes of time in R.A. (=75′) from the on-source position. These spectra were measured along rows where continuum data were taken. After the completion of the spectral line observations, the continuum scans were repeated. To within 10%, there was good agreement between the continuum data taken before and after the spectral line measurements. The positions where spectra were taken are shown as dots in Fig. 1. Over the core of Orion A, the spacing between spectra is mostly 40″, but in some cases a 20″ spacing was used. The FWHP beamsize is shown as a hatched circle in the lower right part of this figure.

We show three spectra in Fig. 2. Within the spectrometer band is the H64α line, and also the He64α and C64α lines. The spectra were analyzed using gaussian fits. In all cases the shape of the H64α line is well represented by a least-squares gaussian fit. However, the helium and carbon lines are blended. In addition the signal-to-noise ratio is much lower for these weaker lines, and in some cases, an instrumental baseline ripple can affect the intensities of such weak features. Given these uncertainties, we have concentrated on the H64α line results.

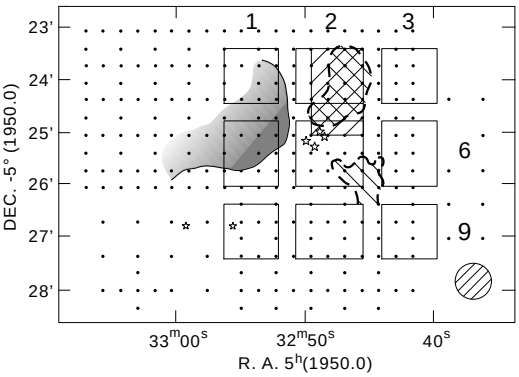

Fig. 1. The dots represent the positions at which H64α spectra were taken toward the core of Orion A. The hatched circle in the lower right represents the 42″ FWHP beam. The four stars near the center of the plot represent the positions of the Trapezium or θ^1 stars. The two stars in the SE represent the θ^2 stars. The shaded region to the NE and E of the Trapezium shows the position of the ′Dark Bay′, a region of foreground extinction. The hatched region N and NW of the Trapezium marks the location of the vibrationally excited molecular hydrogen, hereafter H_2^*; the KL infrared nebula (diameter $< 10''$) is contained within this hatched area. Another hatched area, ∼100″ SW of the Trapezium marks the location of OMC S (also known as OMC1-S or Source 6 of Batrla et al. 1983). As will be discussed later in the text, the numbered rectangles indicate those regions over which we have averaged $T_{\rm e}$ and turbulence values. These results are given in Table 2. The hatched region, which is larger in Declination but smaller in R.A., covers the H_2^* region better. The average over this region allows a more detailed study of any possible connection between ionized gas and the H_2^* outflow surrounding Orion KL.

In Col. 1 and 2 of Table 1, we give the offsets relative to R.A.=05$^{\rm h}$ 32$^{\rm m}$ 48$^{\rm s}$, Dec.=-05$^{\rm o}$ 25′ 23″ (B1950), the nominal peak of the radio continuum (to obtain J2000 coordinates, add +2$^{\rm m}$ 27.4$^{\rm s}$ in α and +2′ 06.7″ in δ). In Col. 3, the LTE electron temperatures, $T_{\rm e}^*$, in Col. 4, the line-to-continuum ratios, in Col. 5, the FWHP linewidths, $\Delta V_{1/2}$. In Col. 6, we list the radial velocities, which are taken with respect to the Local Standard of Rest using the Standard Solar Motion (see, e.g., Allen 1963). To obtain Heliocentric velocities, add 18.3 km s^{-1}. We take turbulent velocities to be the excess line widths after removing the thermal broadening. Since the hydrogen linewidths are found to be gaussian shaped, we can use $V_{\rm turb} = \sqrt{\Delta V_{1/2}^2 - 0.046\,T_{\rm e}^*}$ (see, e.g., Rohlfs & Wilson 1996). The values of $V_{\rm turb}$ are given in Col. 7. In Col. 8, we list the integrated main beam line brightness temperatures. The line-to-continuum ratios, $T_{\rm l}/T_{\rm c}$, were obtained from the peak intensities of the H64α lines divided by the continuum intensities measured at nearly the same time. The radial velocities, $V_{\rm lsr}$, and FWHP linewidths, $\Delta V_{1/2}$ were obtained from gaussian fits to the line spectra.

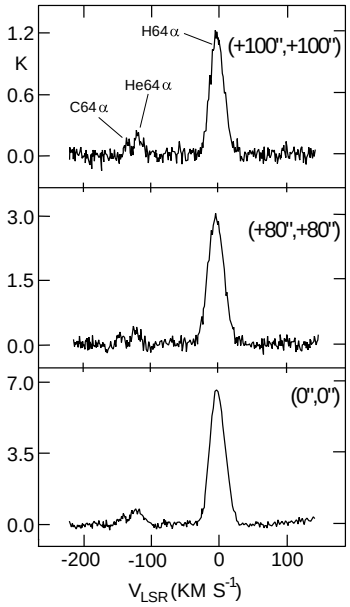

Fig. 2. Three spectra of the 64α lines. The offsets are relative to R.A.=05^h 32^m 48^s, Dec.=-05^o 25′ 23″ (B1950). The most intense feature is the H64α line. The velocity scale is measured for the H64α line (frequency=24.50991 GHz). This velocity is taken with respect to the local standard of rest (LSR), using the standard solar motion. To obtain Heliocentric velocities add 18.3 km s^{-1} (see, e.g. Allen 1963). With respect to hydrogen, the helium line is shifted by -122.2 km s^{-1} and carbon is shifted by -149.6 km s^{-1}. These features are labelled in the uppermost plot.

In Table 2 we list the values and RMS scatter for T_e and V_{turb}, averaged over these regions. To investigate recombination line parameters toward the Orion KL nebula in more detail, we averaged over a second region (shown hatched) which is larger in Declination but smaller in R.A. For this region, the average line parameters are only slightly different from those obtained for Region 2 (in Table 2).

2.2. The 6 cm continuum map

The continuum mapping was carried out in 1989 using the secondary focus 6 cm receiver system in the 100-m telescope, in single feed mode. The center frequency was 4.75 GHz and the bandwidth 500 MHz. The data were taken in excellent weather conditions. The source 3C286 (S=7.5 Jy) served as main calibrator and the sources 3C48, 3C138 and 3C161 were used as secondary calibrators to determine the main beam brightness temperature scale. The HPBW of the 100-m telescope is 2.45′ at 4.75 GHz.

Special observing and data reduction techniques are needed since a high dynamic range image is required. The largest sidelobes are caused by the feed support legs; for Azimuth-Elevation mount telescopes, the position of these sidelobes varies with hour angle, so that the error is a function of time. However, averaged over a 2.45′ beam the Bremsstrahlung emission from an H II region will remain constant during the observing period.

Table 2. H64α line results

Position	T_e^* (10^3 K)	V_{turb} (km s^{-1})
KL/H$_2^*$	8.4±0.5	18.2±0.8
1	7.7±0.6	19.1±0.8
2	8.2±0.5	18.6±0.7
3	8.4±0.9	19.4±1.0
4	8.0±0.9	20.0±1.4
5	8.4±0.4	18.9±1.6
6	8.3±1.4	20.4±0.8
7	8.3±1.2	19.6±0.5
8	8.4±1.0	20.6±2.0
9	9.2±1.0	21.2±1.7

We have made four maps centered on Orion A at different parallactic angles in the Azimuth Elevation coordinate system. The map size was 1.5°×1.5°. The positions of the sidelobes from the strong central source, which appears slightly extended in at the 2.45′ beam, are the same in all these maps. As the first step in our sidelobe correction technique, we used the antenna response from an intense point source, 3C84. We mapped 3C84 using the same procedure as for Orion A, covering a 40′×40′ region. This antenna pattern has been smoothed to the same Gaussian width as measured for Orion A, scaled and subtracted from each of the four individual Orion maps. These four ′cleaned′ maps must then be transformed to the equatorial system. As a second step, the remaining sidelobes, which are less intense and more distant, have been removed following the method described by Reich et al. (1978). Such sidelobes appear in differences between individual maps and the average map, since the maps have been observed at different parallactic angles. The resulting image has a dynamic range of more than 30 dB, or a factor of 10^3 (Fig. 3).

From an integration over a radius of 40′ centered on the peak of the radio continuum, we have determined that the total flux density of NGC1976 and NGC1982 is S(5 GHz)=457±10 Jy. Our flux density value is in good agreement with the lower angular resolution result of Goss & Shaver (1970), S(5 GHz)=472 Jy. If, as expected for optically thin Bremsstrahlung emission (see, e.g., Rohlfs & Wilson 1996, Sect. 9.4), continuum flux density scales as S(ν)=$\nu^{-0.1}$, where ν is frequency, our result is in excellent agreement with the value of S(23 GHz)=400 Jy determined by Wilson & Pauls (1984). Determinations of the flux densities of the individual regions NGC1982 and NGC1976 are more uncertain since these sources are blended. Scaling the 23 GHz continuum map of NGC1982 (Wilson & Pauls 1984) to 5 GHz, we find S(5 GHz)=18 Jy; Shaver & Goss (1970) give a value S(5 GHz)=24 Jy. Subtracting the mean, 21 Jy, from our total flux density, we find that for NGC1976, S(5 GHz)=436 Jy. The estimated RMS uncertainty is 13 Jy. In Fig. 4 we show plots of the continuum intensity versus distance along the two directions marked in Fig. 3.

The mass of ionized gas in Orion A cannot be determined without the use of model calculations. The model of Wilson & Jäger (1987) predicted a total mass (hydrogen mass multiplied by 1.3 to account for helium) of 19 M$_\odot$ out to a diameter of 2.5

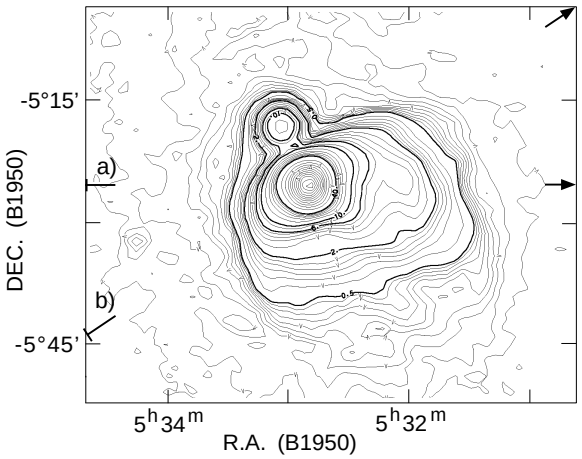

Fig. 3. A 6 cm map of Orion A made with an angular resolution of 2.45′ as described in Sect. 2.2 with a dynamic range of about 1000. (To obtain J2000 coordinates, add +2$^{\rm m}$ 27.4$^{\rm s}$ in α and +2′ 06.7″ in δ). The contours are in units of main beam brightness temperature; the peak value is 330 K. The ratio of main beam brightness temperature to flux density per beam is 2.63. There are two arrows shown. Near the tails, these are labelled **a** and **b**. Starting at the perpendicular lines crossing the tails, we have plotted the continuum intensities as a function of distance, in Fig. 4.

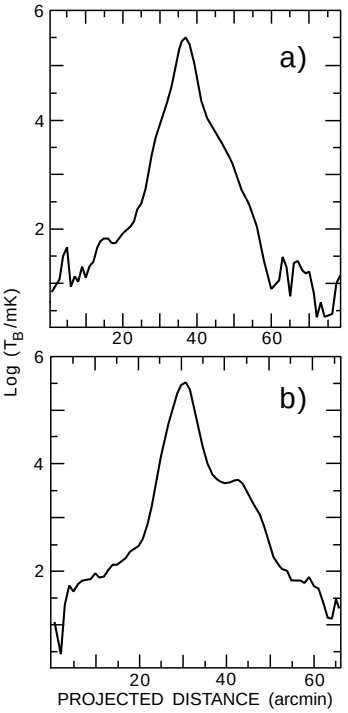

Fig. 4a and b. Plots of the continuum intensity versus distance along two directions labelled **a** and **b**, in Fig. 3.

pc (=17′ at 500 pc). For the 0.5 pc core (=3.4′ at 500 pc), the mass is 1.9 $M_\odot$. Beyond the most extended layer in the model of Wilson & Jäger (1987), our continuum map shows residual emission at the 0.2 K brightness temperature level. If the density in this region is 300 cm^{-3}, the line of sight depth would be 0.02 pc, which yields a mass of ionized hydrogen (with a factor of 1.3 for helium) of 4.7 $M_\odot$. This limit for the ionized gas mass, 24 $M_\odot$, is larger than the *minimum* mass estimate (>5 $M_\odot$) for foreground neutral hydrogen (see Table 5 of van der Werf & Goss 1989). A qualitative estimate for the mass of ionized gas at the edges of Orion A can be made on the basis of optical data. As is well known, optical measurements are more sensitive to ionized gas than radio data. An *upper* limit to the mass of the ionized gas can be had by assuming that the lowest density, very extended part of the optical H II region has an Emission Measure of 50 cm^{-6}pc, density of perhaps 3 cm^{-3} and size of ∼3°. The mass in this layer, which is not in our sensitive radio map, is ∼20 $M_\odot$. All of these values are *much less* than the masses of the exciting stars, which is ∼$10^3 M_\odot$.

3. Discussion

3.1. Electron temperatures

Measurements of the line and continuum intensities, $T_{\rm l}$ and $T_{\rm c}$, together with a value for the FWHP linewidth $\Delta V_{1/2}$, can be used to obtain $T_{\rm e}^*$, the electron temperature, under the assumption of Local Thermodynamic Equilibrium (LTE). For the H64α line the LTE electron temperature, can be obtained from the general formula of Brocklehurst & Seaton (1972):

$$T_{\rm e}^* = \frac{1.84 \cdot 10^5 (N^+/N_e)}{R\, g(T_{\rm e}^*)} \qquad (1)$$

In this expression, R is the ratio of integrated line to continuum intensities, N_e (=H$^+$ and He$^+$) and N^+ are the electron and ion (=H$^+$) densities. The Gaunt factor, g, is $g(T) = \frac{3}{2}\log T - 2.66$. Thus the value of $T_{\rm e}^*$ depends only on directly measured quantities. This has a great advantage, since with a set of spectral line and continuum measurements, one could determine the LTE electron temperature of an HII region. $T_{\rm e}^*$ can be related to the actual value, $T_{\rm e}$, using model calculations. From Brocklehurst & Seaton (1972), the equation relating $T_{\rm e}^*$ to $T_{\rm e}$ is given by

$$T_{\rm e} = bT_{\rm e}^*(1 + \frac{1}{2}(1-\beta)\tau)\frac{g(T_{\rm e}^*)}{g(T_{\rm e})} \qquad (2)$$

where, following Brocklehurst (1970), b is the departure coefficient and

$$\beta = 1 - (\frac{kT_{\rm e}}{h\nu})(\frac{d\ln b}{dn}). \qquad (3)$$

β depends on the difference of b values in the upper and lower levels of a transition. The total optical depth $\tau = \tau_{\rm l} + \tau_{\rm c}$, is the sum of the line and continuum optical depths.

For the core of Orion, Pauls & Wilson (1977) and Seaton (1980) found that the line masering and level population corrections nearly balance for transitions at 1.3 cm. An examination of the numerical values for the right side of (2) is useful. For the 2.5′ diameter dense core of Orion A, one has an RMS electron density of $\langle N_{\rm e}\rangle = 5 \cdot 10^3$ cm^{-3}, and $T_{\rm e}^*$ of 8200 K. At 23 GHz, the continuum optical depth, $\tau_{\rm c}$, is more than five times the line optical depth, and so dominates the value of τ in (2). If there is no significant fine scale structure, we can estimate $\tau_{\rm c}$ from the map of Wilson & Pauls (1984). Taking

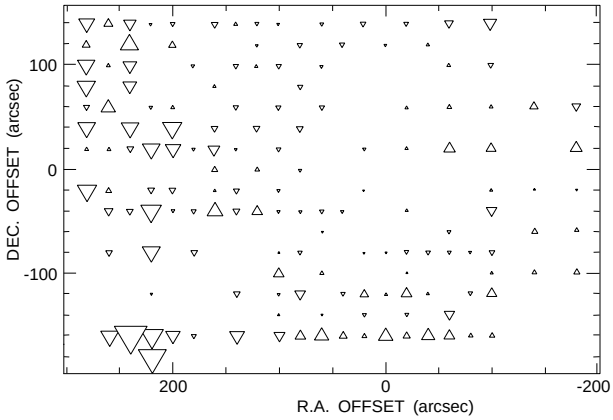

Fig. 5. The distribution of the difference between the individual values of electron temperature and the average value, 8300K, for the positions measured in the core of Orion A (see Table 1). An upward pointing diamond indicates a value larger than the average, while a downward pointing diamond a value lower than the average. For the H64α line averaged over a 42″ beam, T_e^* is very nearly T_e, so we have used T_e^* for the value of the the actual electron temperature.

T_e=8300K, we find that $\tau_c = 3.7 \cdot 10^{-3}$. From the tabulations of Brocklehurst (1970), we have for the H64α line, the departure coefficient is $b_{64} = 0.99$ and the line masering coefficient is $\beta_{64} = -42$. Then $T_L = 1.07\,T_L^*$, and the LTE value of T_e represents the actual value of T_e very well. Thus, for the core of Orion A, $T_e \approx T_e^*$. We take these two quantities to be equal in the following discussions.

In Fig. 5 we show a plot of the deviation of T_e from the average over the region mapped. From this plot and Tables 1 and 2, there is little deviation from the average values of T_e^* over the H_2^* region. The average values of T_e in Table 2 lie between 7700K and 9200K with a typical scatter of 500 to 1300K. Since we have repeated our measurements on different days, and interspersed line and continuum measurements, we are rather confident that our results are not greatly affected by systematic errors. However, the fact that the lowest value of T_e is in the SW and the highest value in the NE of the core of Orion A indicates that there may have been a $\sim$10″ misalignment of the line and continuum maps. Such an effect would cause apparent small gradients in T_e even if the actual T_e in a region was constant. A related question is whether there is a significant scatter in the T_e values between individual positions. From Fig. 5 and Table 2, there are definitely differences in T_e with spatial location. In a single velocity channel, this noise is less than 5% of the peak line intensity, even for the weakest lines. However, there might be systematic errors in the setting of the zero levels in the frequency baselines, and a misalignment of the continuum scans and the positions at which the spectra were taken. Thus, the scatter in Table 1 and Table 2 is *not* larger than the scatter one would estimate from the RMS noise in the spectra. Then, we find *no* evidence for changes in T_e from position to position in the core of Orion A.

3.2. Comparison with previous results

Our data in Table 1 is in good agreement with the H76α line results of Pankonin et al.(1979) and the H64α line data Pauls & Wilson (1977). Based on their H51α line data, at a wavelength of 7mm, Hasegawa & Akabane (1984) had reported recombination line emission with a large linewings than emission from the HII region. From these data, they estimated that T_e^* was $\sim$3.5 10^3K over a $\sim$1′ region. We have averaged over a similar region (shown hatched in Fig. 1); we find *no* evidence for large linewings or excess emission, neither in our individual spectra nor in our averages. This indicates that there is only little recombination line emission from the Orion KL outflow provided that the 1.3 cm and 7 mm emission samples the same region.

The second hatched area in Fig. 1, $\sim$100″ south of the Orion KL region, is Source 6 of Batrla et al. (1983), otherwise known as OMC S. From the 6 cm H_2CO line maps of Johnston et al. (1983) and Mangum et al. (1993), the maximum absorption line temperature exceeds the temperature of the microwave background. Thus Johnston et al. (1983) concluded that this region is in front of a continuum source. Since there is no compact source detected with the VLA, the background source must be extended. The simplest conclusion is that the molecular region seen in H_2CO must be inside the boundary of this source. However, there seems to be no large deviation from the average values of line parameters in this region. With one exception, our average values for T_e are the same as those obtained from new measurements of the Balmer jump by Liu et al. (1995). The one difference is for an EW slit position, which is 7200K. This difference is surprising since the weighting of T_e values from recombination lines and the Balmer jump are the same. Liu et al. (1995) had noted that the optical Balmer jump emission may arise from a lower ionization region with a lower T_e value. O'Dell (priv. comm.) comments that there seems to have been no correction for reddening, and the EW slit position data may have been affected by higher extinction from foreground material in the ′Lid′ (see our Fig. 7).

3.3. Element abundances and T_e values

Many different measurements have shown that Orion A is *underabundant* in oxygen compared to the solar system (see, e.g., Mathis 1997). Peimbert & Torres-Peimbert (1977) had argued that T_e fluctuations which will raise the O/H ratio. The optical value of T_e as obtained from the O^{++} forbidden line ratio (see, e.g., Seaton 1980 or Rohlfs & Wilson 1996, Eq. 13.5) are biased toward higher values of T_e, while Balmer jump or radio recombination line data are biased toward lower values of T_e. Thus, any systematic differences in these T_e values would indicate that fluctuations are present. Our results and those of Liu et al. show excellent agreement with optical determinations Peimbert & Torres-Peimbert (1977). Thus *there are no significant temperature variations on 40″ scales*. This indicates that the RMS mean squared temperature fluctuations are small. This good agreement should settle the issue of T_e fluctuations. However, Peimbert et al. (1993) have adduced additional evidence

for T_e fluctuations from differences in oxygen abundances determined from optical data for oxygen for recombination lines and forbidden lines. These results are in disagreement with the previous data, and these differences are *not* understood.

There is additional, indirect, evidence that T_e fluctuations cannot be large. First, models of nebulae by Kingdon & Ferland (1995) show that none of the models give T_e fluctuations large enough to reconcile the optical oxygen recombination line data with the oxygen forbidden line results. Second, Edvardsson et al. (1993) have shown that low mass stars in the solar neighborhood also have higher O/H ratios than the solar system. Thus, the ′oxygen anomaly′ in Orion A may actually be caused by anomalous solar system abundances and is *not* due to T_e fluctuations in Orion A. The birthplace of the solar system may have been 2 kpc closer to the galactic center (Wielen et al. 1996, Wielen & Wilson 1997), or the solar system abundances may have been anomalous. The case for anomalies is supported by meteoritic data (see, e.g., Nittler et al. 1996).

3.4. Turbulent velocities

In Table 2, we list the turbulent velocities, averaged over the regions shown in Fig. 1. In Fig. 6 we show the distribution of V_{lsr}'s over the same region. These plots illustrate two important observational facts:
(1) The values of $\Delta V_{1/2}$ do not vary by more than 5% over the region mapped, and
(2) The radial velocities change very significantly.

The values of T_e are also constant over the region mapped, so the turbulent velocities will not vary; these are larger than 10 km s^{-1} in all cases. It is not clear how such large values can be maintained over long times if the gas is fully ionized (Münch 1958). One might suppose that the turbulence we measure is merely caused by the averaging over 0.1 pc regions in our large beam. However, from optical studies for angular scales of 3″, (Castaneda 1988, O'Dell & Wen 1992) finds that the excess line broadening in optical spectra is ∼8km s^{-1} also. Ferland (priv. comm.) notes that the broadening might be due to Alfvén waves if the magnetic field strength is a few hundred μGauss (see Eq. 14.114 in Rohlfs & Wilson 1996).

An estimate of the power which could contribute to turbulent motions can be obtained from an analysis of flows off neutral matter which is ionized at the boundaries. In the case of Orion A, this would be material in fronts at the rear face adjoining the molecular cloud behind the HII region, the Dark Bay to the NE (see Fig. 1) and/or the neutral lid in the foreground (Wen & O'Dell 1995, van der Werf & Goss 1989). The power is ∼1 L$_\odot$. If the time scale for dissipation is 10^3 years, the observed turbulent energy could be accounted for. However, the dissipation time is uncertain, and the turbulence must be transported to the interior of the H II region. Another estimate for the turbulence input in the interior of the H II region might be had by an estimate of flows off embedded neutral clouds (Garay et al. 1987, Churchwell et al. 1987). Using HST data, O'Dell & Wen (1994), have found 55 young stars in Orion A which are surrounded by circumstellar material; Stauffer et al. (1994) find similar concentrations. Following O'Dell & Wen, such ′proplyds′ are thought to have masses of 10^{28} gm. Wilson & Jäger (1987) estimated that the core of Orion A, to a diameter of 0.5 pc, has a mass of 1.9 M$_\odot$. If we assume that all of the gas in the core is turbulent and that this turbulence is dissipated in $< 10^3$ years, there would have to be a mass flux of $>4\ \ 10^{30}$ g yr^{-1}. If this mass were supplied *only* by proplyds, >400 would have to be evaporated per year. This seems to be much larger than the total number one would expect to find in Orion. Thus the origin of the turbulence is not likely to be proplyds alone.

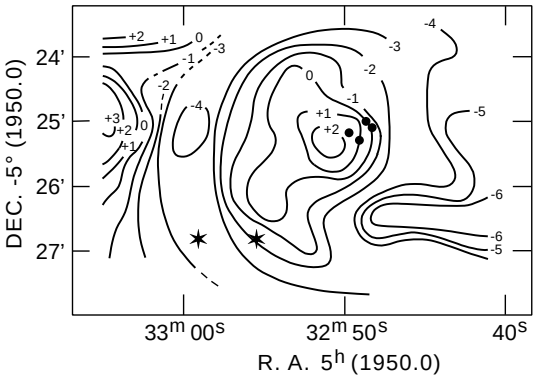

Fig. 6. A contour map of the V_{lsr} radial velocity distribution in km s^{-1} for the core of Orion A. This plot is based on gaussian fits to the H64α line spectra. The numerical results are given in Table 1.

3.5. Radial velocity distribution

The V_{lsr} of the ionized gas is negative compared to the V_{lsr} of the background molecular cloud, +7 km s^{-1} to +9 km s^{-1}. The most positive V_{lsr} values are found ∼0.5′ and 4′ east of the Trapezium stars. The maximum closer to the Trapezium is extended to the SE. This extension of gas at 0 km s^{-1} follows the shape of the continuum contours which outline the bright bar of emission in Orion.

There is good agreement between our results and the data of Pankonin et al. (1979). Our larger sample of V_{lsr} data were taken with a better angular resolution and cover a larger region. First, we compare our results with optical data. Castaneda (1988) and Wen & O'Dell (1993) have analyzed optical spectra of Orion A, grouping the results into 4 systems: A high flux system (A), a low velocity system (B), a broad line system (C), and a high velocity system (D). O'Dell (priv. comm.) has informed us that: (1) Systems A and B are likely to be directly related; (2) System A arises from the ionization front abuting the Orion molecular cloud, where the densest gas is present; (3) System B is a component in System A flowing toward the observer, but not a separate velocity component (O'Dell & Henney, priv. comm.), (4) System C is probably the result of scattered line radiation. There is a reasonable agreement with the radial velocities of the [SIII] lines with the highest fluxes in ′System A′ of O'Dell & Wen (1993). There is agreement between all of these results in that toward the Trapezium the radial velocities are the most positive, and the radial velocities become more negative to the East and West of the Trapezium. Our more extensive data (Fig. 6) shows

that between 0.9′ and 3′ to the West of the Trapezium the radial velocities become more negative, while at 2.7′ East of the Trapezium there is a negative velocity region, and further to the East, the radial velocity becomes more positive.

In a simple picture of ′champagne flow′ (see, e.g, the discussion in Pankonin et al. 1979), one would expect that the radial velocities of the ionized gas are determined by the flow off the molecular cloud behind the HII region. Then the ionized gas has a radial velocity which is more negative than that measured for the neutral gas. This is certainly the case for the radial velocity averaged over the entire source, since the $V_{\rm lsr}$ of the molecular cloud is $\sim$8km s^{-1}. However, on a fine scale the motions are more complex than expected on the basis of a simple flow. Pankonin et al. (1979) extended the simple champagne flow model by supposing that there is a strong wind from the Trapezium stars, creating a cavity around the Trapezium. This cavity is an obstacle for the flow of ionized gas toward the observer. This extension can explain the 'negative–positive–negative' trend in radial velocity near the Trapezium. In addition, the continuum maximum and the peak of the radial velocities will not coincide with the Trapezium stars if we are viewing Orion A from an angle. The positive $V_{\rm lsr}$ values toward the Bright Bar would indicate that the lower density cavity around the Trapezium must extend to the SE, but not SW of the Trapezium. There are a number of molecular features to the SW of the Trapezium: The OMC S and its outflow, as well as a neutral region inside the boundaries of the ionized gas region. The outflow from OMC S to the SW is highly collimated but the NE part of such an outflow is missing. This NE outflow may be blocked by the presence of ionized gas. If so, OMC S is interacting directly with the HII region. The negative velocity contours may be a sign of this interaction. In addition to the molecular features, Jaffe & Pankonin (1978) have found a maximum in the C109α carbon recombination line emission at $V_{\rm lsr}$=8.5km s^{-1} to the SW of the Trapezium, indicating a high column density interface between the ionized and molecular gas in this direction. As pointed out by Johnston et al. (1983) and confirmed by Mangum et al. (1993), a part of the S6 region (the region SW of the Trapezium, shown shaded in Fig. 1) must be *inside* the HII region. As noted by O'Dell (priv. comm.), there are a number of dark features and filaments very close to the OMC S/S6 region. A search for deeply embedded sources and an investigation of H_2O masers in this region has been carried out by Gaume et al. (1997).

3.6. Refinements to the models of Orion A

In agreement with previous authors, we find that the simplest explanation for the spatially extended negative velocity gas to the west of the Trapezium is a free flow of ionized material toward us. Toward the east of the Trapezium, the situation is different. Our 6 cm map clearly shows a sharp fall off of the continuum emission to the east (see Figs. 3 and 4). It is possible that the fall off is even sharper, but that we are viewing the boundary of ionized and neutral gas at an angle. The new fact to be explained is the positive value of $V_{\rm lsr}$ further to the east. There are two possible models. In the first model, the $V_{\rm lsr}$ variations reflect the angle between the normal to the interface of the HII region with the neutral background cloud and our line of sight. Then the ′positive-negative-positive-negative′ trend in $V_{\rm lsr}$ requires the presence of a cusp at the location of the Trapezium stars, with the background ionized-neutral interface curving away from the stars to the east and west of the location of the cusp. The optical Dark Bay plays no role in determining the variation of $V_{\rm lsr}$. The second model is more complex, in that the Dark Bay must be close to Orion A and plays a large role in establishing the variation of $V_{\rm lsr}$. In this picture, the positive $V_{\rm lsr}$ is caused by the flow of ionized gas off a foreground neutral boundary. In this model, the boundary in the east wraps around the ionized gas, but is at an angle of perhaps 30$^{\rm o}$ to the line-of-sight. The eastern-most edge of the dark bay must be at about the projected distance, $\sim$0.7pc, from the Trapezium. Averaged over all Declinations, the linewidths in the East are 3%, or 0.6 km s^{-1} larger than in the West. In addition, Jaffe & Pankonin (1978) also found a C109α maximum in the East near the Dark Bay position.

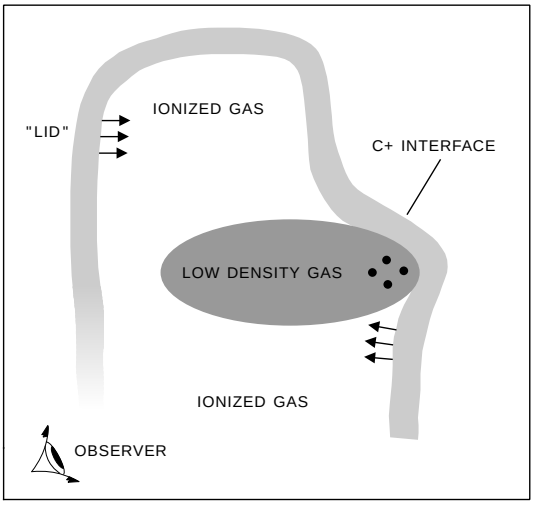

Fig. 7. A sketch of the core of Orion A, as seen from above. The arrows show the direction in which gas is flowing off neutral surfaces.

On the basis of the present radio astronomical data, we prefer the second model described in the previous paragraph. In Fig. 7 we show a sketch of the structure which we propose for Orion A. This is an extension of the models proposed by Balick et al. (1974), Pankonin et al. (1979), Simpson et al. (1986), van der Werf & Goss (1989) and Felli et al. (1993). This mostly deals with details outside the 0.9 pc region modelled by Wen & O'Dell (1995). The Trapezium stars are located in a small region at the rear of the HII region (Pankonin et al. 1979, Simpson et al. 1986). To the East, foreground neutral gas causes extinction. We assume that dense gas near the ionizing star shields the more distant gas in the East from the flux of ionizing photons, so the positive $V_{\rm lsr}$ in the East would be a flow off this foreground neutral gas. This dense neutral region halts the expansion of the HII region to the East. To the West, there is less dense neutral matter, so the ionized gas can flow more freely. These structural modifications should not affect the radio recombination line models too greatly. At the short cm wavelengths, there is

little stimulated emission, and the geometric details are not very critical. At longer cm wavelengths, the details of geometry *are* important, but single telescope data averages over the entire source. These averages are rather weak functions of the fine scale size changes we propose (see, e.g., Wilson & Jäger 1987). Interferometer maps show no radio continuum emission from this foreground ionized gas (Johnston et al. 1983, Yusef-Zadeh 1990, Felli et al. 1993); such emission may have little fine scale structure, and thus would not be recorded. This model can be tested using higher angular resolution images of the hydrogen recombination line emission of this region.

In agreement with previous authors, we interpret the structure of Orion A in terms of the flow off a massive neutral background cloud. There is a free expansion of the ionized gas in the west, but a neutral boundary in the east.

4. Conclusions

Based on our 42″ resolution mapping of the core of Orion A in the H64α line at 24.5 GHz, we conclude that:

(1) Our $V_{\rm lsr}$ mapping results support the data of Pankonin et al. (1979), in which there is a minimum toward the Trapezium. Our more extensive data shows an increase in $V_{\rm lsr}$ at $\sim$4′ to the east. Thus from west to east, through the position of the Trapezium, the $V_{\rm lsr}$ varies from -5km s^{-1} to +2 km s^{-1} to -4 km s^{-1} to +3 km s^{-1}.
(2) We find no significant differences in either electron temperature, FWHP linewidth, $\Delta V_{1/2}$, or $V_{\rm lsr}$ toward the Orion KL nebula, the H_2^* region or the OMC S outflow source.
(3) On the basis of our H64α line data and our 6cm continuum map, we propose a refinement to previous models. In our picture, to the east the more positive $V_{\rm lsr}$'s may result from a flow of ionized gas off a foreground neutral region which obscures the HII region. We assume that ionized gas can flow more freely to the west. We view Orion A from the west, so the $V_{\rm lsr}$'s in the western part of the source are more negative.
(4) Model calculations show that at 1.3 cm, $T_{\rm e}^*$, obtained directly from measurements, is equal to $T_{\rm e}$. A search for cold ($T_{\rm e}$ $\sim$3000K) ionized gas toward the KL nebula produced a negative result. Our average $T_{\rm e}$ is 8300$\pm$200K. There is no significant difference between $T_{\rm e}$ values determined from radio recombination lines and those determined from forbidden optical lines of [O III]. There is also good agreement with the Balmer decrement data, except for one position where either the Balmer decrement measurement refers to a low excitation region or there is an inadequate correction for extinction.
(5) From our radio continuum data and detailed quantitative models of the H II region, the total mass of H II (scaled upward by 1.3 to account for He) in Orion A is 24 $M_\odot$. In the 3′ diameter core, the mass is 1.9 $M_\odot$.

Acknowledgements. We thank Prof. C.R. O'Dell, presently at MPIfA Heidelberg, M. McCaughrean, and C.M. Walmsley for useful discussions. C.R. O'Dell also served as the referee.

References

Allen, C.W. Astrophysical Quantities, 2nd ed. 1963 Athlone Press, p. 242
Balick, B., Gammon, R.H., Hjellming, R.M. 1974 PASP 86, 616
Batrla, W., Wilson, T.L., Bastien, P., Ruf, K. 1983 A & A 128, 279
Brocklehurst, M. 1970 MNRAS 148, 417
Brocklehurst, M., Seaton, M.J. 1972 MNRAS 157, 179
Castaneda, H.O. 1988 ApJS 67, 93
Churchwell, E.B., Felli, M., Wood, D.O.S., Massi, M. 1987 ApJ 321, 516
Edvardsson, B., Andersen, J., Gustafsson, B., Lambert, D.L., Nissen, P.E., Tompkin, J., 1993 A & A 275, 101
Felli, M., Churchwell, E.B., Wilson, T.L., Taylor, G.B. 1993 A & AS 98, 137
Garay, G., Moran, J.M., Reid, M.J. 1987 ApJ 314, 535
Gaume, R.A., Wilson, T.L., Vrba, F.J., Johnston, K.J., Schmid-Burgk, J. 1997 ApJ submitted
Goss, W.M., Shaver, P.A. 1970 Austral J Phys Suppl 14, 1
Hasegawa, T., Akabane, K. 1984 ApJ 287, L91
Hayward, L.T., Houck, J.R., Miles, J.W. 1994 ApJ 433, 157
Jaffe, D.T., Pankonin, V. 1978 ApJ 226, 869
Johnston, K.J., Palmer, P., Wilson, T.L., Bieging, J.H. 1983 ApJ 271, L89
Kuiper, T.B.H., Evans, N.J. II 1978 ApJ 219, 141
Kingdon, J.B., Ferland, G.J., 1995 ApJ 450, 691
Liu, X.-W., Barlow, M.J., Danziger, I.J., Storey, P.J. 1995 ApJ 450, L59
Lockman, F.J., Brown, R.L. 1975 ApJ 201, 134
Mangum, J.G., Wootten, A., Plambeck, R.L. 1993 ApJ 409, 282
Mathis, J.S. 1997 ApJ submitted
McCaughrean, M., Stauffer, J.R. 1994 AJ 108 1382
Münch, G. 1958 Rev. Mod. Phys. 30, 1035
Nittler, L.R., Amari, S., Zinner, E., Woosley, S.E., Lewis, R.S. 1996 ApJ 462, L31
O'Dell, C.R., Wen, Z. 1993 ApJ 409, 262
O'Dell, C.R., Wen, Z., Hu, X. 1993 ApJ 410, 696
O'Dell, C.R., Wen, Z. 1994 ApJ 436, 194
Osterbrock, D. E., Tran, H.D., Veilleux, S. 1992 ApJ 389, 305
Pankonin, V., Walmsley, C.M., Harwit, M. 1979 A & A 75, 34
Pauls, T., Wilson, T.L. 1977 A & A 60, L31
Peimbert, M., Torres-Peimbert, S. 1977 MNRAS 179, 217
Peimbert, M., Storey P.J., Torres-Peimbert, S. 1993 ApJ 414, 626
Pogge, R.W., Owen, J.M., Atwood, B. 1992 ApJ 399, 147
Reich, W., Kalberla, P., Reif, K., Neidhöver, J. 1978 A & A 69, 165
Rohlfs, K., Wilson, T.L. 1996 'Tools of Radio Astronomy', 2nd ed. Springer-Verlag, Heidelberg
Seaton, M.J. 1980, 'Theory of Recombination Lines', in P.A. Shaver(ed) Radio Recombination Lines, Reidel, Dordrecht, p. 3
Shaver, P.A., Goss, W.M. 1970 Austral J Phys Suppl 14, 133
Shaver, P.A. 1980 A & A 90, 34
Simpson, J.P., Rubin, R.H., Erickson, E.F., Haas, M.R. 1986 ApJ 311, 895
Stauffer, J.R., Prosser, C.F., Hartmann, L., McCaughrean, M. 1994 AJ 108 1375
van der Werf, P.P., Goss, W.M. 1989 A & A 224, 209
Wen, Z., O'Dell, C.R. 1995 ApJ 438, 784
Wielen, R., Fuchs, B., Dettbarn, C. 1996 A & A 314, 438
Wielen, R., Wilson, T.L. 1997 A & A (in press)
Wilson, T.L., Pauls, T. 1984 A & A 138, 225
Wilson, T.L., Jäger, B. 1987 A & A 184, 291
Yusef-Zadeh, F. 1990 ApJ 361, L19